

[\[Print Version\]](#)

[\[PubMed Citation\]](#) [\[Related Articles in PubMed\]](#)

## TABLE OF CONTENTS

[\[INTRODUCTION\]](#) [\[MATERIALS AND...\]](#) [\[RESULTS\]](#) [\[DISCUSSION\]](#) [\[CONCLUSIONS\]](#) [\[REFERENCES\]](#) [\[TABLES\]](#) [\[FIGURES\]](#)

*The Angle Orthodontist*: Vol. 76, No. 4, pp. 605–611.

# Accuracy of Facial Plaster Casts

## *A Three-dimensional Scanner Study*

Christof Holberg;<sup>a</sup> Katja Schwenzer;<sup>b</sup> Luai Mahaini;<sup>c</sup> Ingrid Rudzki-Janson<sup>d</sup>

### ABSTRACT

**Objective:** The aim of this study was to evaluate the accuracy of facial plaster casts and their suitability for 3-D mapping.

**Materials and Methods:** All measurements were carried out on 15 adult probands (seven female and eight male; age range 19–31 years, mean 24.7 years). A plaster cast of the facial surface was prepared for all probands using alginate impressions. The plaster casts and the probands faces were digitized using a three-dimensional laser-scanner operating with structured light. The resulting point clouds were matched in a virtual environment to analyze the deviations between the cast and the facial surfaces, both qualitatively and quantitatively.

**Results:** The average deviations depended on the facial area and lay between 0.95 and 3.55 mm. Marked differences between the plaster cast and the facial surface were found, particularly in the area of the lips, at the roof of the nose, at the cheeks, and in the entire lower facial area.

**Conclusions:** The regionally exacerbated soft tissue deformations that occur during impression of the facial surface lead to inaccuracies in the resulting plaster cast that forbids any use for morphometric analysis. Documentation of pathological findings in cleft lip and palate using facial plaster casts does appear to be justifiable.

**KEY WORDS:** Facial plaster cast, Facial impression, Facial surface, 3-D scanner, Cleft lip palate, Facial mapping.

Accepted: July 2005. Submitted: April 2005

### INTRODUCTION [Return to TOC](#)

An important aspect of orthodontic diagnostics is the recording of facial soft parts for documentation and the analysis of facial esthetics. Most traditional soft tissue records such as photography<sup>1</sup> have been two-dimensional, but the possibility also exists to record the facial surface in three dimensions. This can be performed either by generating facial plaster casts<sup>2</sup> after alginate impression or by digitalization of the facial surface using three-dimensional (3-D) scanners. Digital face recording benefits from the fact that it is contact free, but the 3-D scanners required are very expensive and are available only at specialized research centers.<sup>3</sup>

In contrast, manual impressions of the face represent an easy to handle low-cost procedure, which have already long been applied successfully for the documentation of cheilognathopalatoschisis,<sup>4</sup> the production of epitheses,<sup>5–8</sup> and for radiooncology.<sup>9</sup> The plaster face casts resulting from alginate impressions are not just virtual (unlike the 3-D scanner procedure) but are in fact real, so they can be measured using a vernier scale. However, a key disadvantage of alginate impression is the deformation of soft tissue parts that occurs during impression because the procedure is not contact free.



No information has been published previously in the literature regarding the extent and direction of such deformations. The objective of this study was to assess this deformation error<sup>10</sup> qualitatively and quantitatively and to clarify whether low-cost facial impression using alginate represents a sufficiently precise alternative to digital face recordings that involve 3-D scanners.

## MATERIALS AND METHODS [Return to TOC](#)

All measurements were carried out on 15 adult probands (seven female and eight male; ages 19–31 years, mean 24.7 years). Before starting the study, the procedures were explained to each proband, and a letter of agreement was signed. The university approved all study conditions. Each proband laid flat on a dental chair, and the facial surface was modeled using alginate. Using this impression, an individual plaster cast was prepared that served as the basis for all further measurements. After protecting the hair with a stocking ribbon and greasing the eyebrows with Vaseline, respiration was safeguarded using small plastic tubes that were placed either in a nostril (12 individuals) or between the lips (three individuals) if nasal respiration was impaired in these individuals.



The contacting alginate (Bayer Inc, Leverkusen, Germany) was applied over the entire facial surface of the individual while checking for a bubble-free covering of the nose, mouth, and eyes. Bent paper clips were inserted in the alginate layer to serve as retention aids for a subsequently applied layer of alabaster intended to strengthen the alginate impression material. Any inadvertent obstruction of the respiration tubes by the plaster had to be avoided at all costs.

After the alabaster-strengthened impression was set, it was removed from the face together with any loose alginate and plaster pieces. The alabaster-strengthened alginate impression was filled with hard plaster, and a plastic bottle was introduced as a spacer for reducing the weight of the subsequent plaster cast. The plastic bottle was removed after the cast was set, then the alabaster-strengthened alginate impression material was fractured with a hammer, and any remaining plaster edges of the cast were removed carefully using a milling cutter.


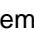

The surface of the plaster cast was digitized using a 3-D scanner ([Figure 1](#) ). Because the facial surfaces of the individuals were also directly digitized, the “matching” point clouds could be overlaid in the computer, and the differences could be quantified. The digitization of all facial surfaces and plaster casts was carried out using a light-coded triangulation procedure (Tricolite®, Steinbichler Inc, Neubeuern, Germany) which operates with structured light and uses a phase shift to increase the precision effect ([Figure 2](#) .

During data acquisition, several white strips were projected onto the object to be measured. These strips were then recorded using two charged coupling device (CCD) cameras from different visual angles. The distance between the projector and the cameras to the measured object was 0.8 m. The projector was placed in the central axis, and the two CCD cameras were placed at 30° angles. The projection of the strip-light sequences was carried out using computer-controlled liquid crystal display (LCD) masks that were controlled horizontally and vertically by the Comet® program (Steinbichler). Both CCD cameras used for data acquisition were calibrated before the start of measurements to guarantee a precise coordinate recording by the triangulation principle.

All measured objects (individuals, plaster casts) had to be positioned before the 3-D scanner so that all surfaces could be covered simultaneously by the projector and the CCD cameras and geometric undercuts avoided. On illumination of the measured objects, areas prone to shadowing, eg, next to the nose or under the chin, received special attention.

After calibration and exact positioning of the measured object, the scan process was run in a sequence controlled by the Comet® program (Steinbichler). The quantitative recording of the brightness distribution on the measured object ([Figure 3](#) ) followed the identification of the object boundaries, the implementation of the phase shift, and the triangulation measurement ([Figure 4](#) ) all steps that took 1–2 seconds in all.

All acquired 3-D coordinate data were filtered in the Comet® program, and redundant points eliminated for more efficient data evaluation. The quantitative measurement of all deviations between the facial surface and the plaster cast was carried out using the Surfacer® program (Metrix Software Solutions Ltd, Montreal, Canada) into which all the raw data acquired was imported. In this software, which has found widespread application particularly in the automobile industry, the two point clouds can be analyzed and measured at leisure.

However, in advance, the acquired facial surfaces had to be digitally laid over the record of the corresponding plaster casts in the virtual environment. This process, termed matching, was carried out using a special algorithm that positioned both point clouds in such a way that the sum of all individual distances was as small as possible ([Figure 5](#) ). The horizontal and vertical sectioning which was then carried out ([Figure 6](#) ) through both point clouds allowed an interactive measurement of discrepancies between the plaster cast and the facial surface for individually defined measuring points<sup>11</sup> (localization and definition are shown in [Table 1](#) ). Finally, all data obtained were entered into the software SPSS version 10.0 (SPSS, Chicago, Ill) for statistical analysis. This was a descriptive statistical analysis,

whereby all differences between the plaster cast and the facial surface were evaluated. The value of difference and its vector were registered for each anatomical measurement point before the values were evaluated descriptively (mean, maximum, minimum, and standard deviation).

## RESULTS [Return to TOC](#)

The average discrepancy between the plaster cast and the facial surface was 2.3 mm (n = 165; 11 measuring points with 15 plaster casts). The integral and direction of the error vector revealed a marked location dependency. The duplication precision of the plaster cast was highest in the upper third of the face (forehead and nasal base). In this study, average errors of between 1 mm (forehead) and 1.4 mm (nasal base) were measured ([Figure 7](#)). The cheek area followed with a mean error of 2.1 mm (n = 30), with slight differences between the two facial halves: 1.8 mm (n = 15) on the left and 2.3 mm (n = 15) on the right. At the subnasal measuring point, the mean deviation of the plaster models was 2.3 mm, whereas at the upper lip it was 2.9 mm and at the lower lip it was 2.8 mm. Mean deviations (n = 15) of more than 3 mm were registered at the nasal tip (3.2 mm), the soft pogonion (3.6 mm), and the soft menton (3.4 mm). All individual measurements from the 15 probands are shown in [Table 2](#).

In addition to the integral of the error vector, the dominant vector direction was also determined at the individual measuring points. After impressing with alginate, the nasal tip had been deformed caudally in seven cases, cranially in three cases, and posteriorly in another three cases. In two plaster casts, no clear direction of the error vector could be recognized (see [Table 3](#)). At the soft tissue pogonion, the direction of the error vector was posterior in nine cases, cranial in four cases, and caudal in two cases. However, soft tissue menton was cranial in 13 cases and caudal in only two cases ([Table 3](#)). The cheeks in most cases were deformed medially. However, the subnasal area and the upper and lower lips were usually compressed posterior, cranial, or caudal. The error vectors at all remaining measuring points showed no irregularities and are also listed in [Table 3](#).

During impressing, respiration was safeguarded using a small nasal tube for nine probands, whereas three individuals received a small oral tube. The mean integral of the error vector in the individuals who respired orally was 3.2 mm, and as such was far higher than that observed in the nasal-respiring individuals (2.1 mm). Particularly, high error values occurred amongst the oral breathers at the measuring points of the upper lip, the lower lip, the soft pogonion, and the soft menton. The different results depending on tube positioning are illustrated in [Table 4](#).

## DISCUSSION [Return to TOC](#)

These results show that an impression of the face with alginate can cause between 1 to 3 mm of soft tissue deformation. The resulting impression errors are especially evident in areas that are important for the assessment of facial esthetics (lower facial third, nasal tip, subnasal region, and cheeks). The impression errors at the forehead, glabella, and nasal base, on the other hand, were moderate (an average of 1 mm).

In orthodontics, facial plaster casts are used for the 3-D mapping of pathological soft tissue lesions, such as those usually observed in cleft lip and palate or in syndrome patients.<sup>4</sup> Also, the use of casts as a basis for 3-D soft tissue analysis seems to represent a reasonable pursuit. On the basis of our results on the precision of facial plaster casts, it can be concluded that facial plaster cast use merely for documentation and visualization purposes appears reasonable and practical. However, problems arise with morphometric measurement and analysis of the plaster casts leading to inaccurate results and false esthetic conclusions.

Casting of facial soft tissue parts with alginate represents a simple and low-cost procedure, but more expensive 3-D scanner systems<sup>12-17</sup> are much more accurate because they make no contact with, and so do not deform, the object being measured. However, with alginate impression of the facial soft tissue areas, deformation artifacts preferentially affect only regions that are inadequately supported, such as the nasal tip, or that have a substantial soft tissue layer, such as the lips and the cheeks. In contrast, areas that feature a thin and well-supported (by hard tissue) soft tissue layer such as the forehead are depicted by alginate without any considerable deformation.

Because casting of the face was carried out while the individuals were prone, the influence of gravity must also be considered when judging the results. This might explain the large inaccuracies observed in the area of the soft pogonion and menton because there the error vectors were usually in the dorsal direction.

Movement artifacts caused by breathing during alginate impressing led to large inaccuracies particularly in the areas of the lips and the nose. The use of oral respiration tubes led to greater deformations than was observed with the use of nasal tubes ([Table 4](#)), probably because of amplified lip movements. However, in this study, it must be considered that there was a major imbalance in the number of individuals who were nasally and orally ventilated (12 to three, respectively), so that only a very cautious interpretation of the results was possible. To reduce such movement artifacts, respiration should not be assisted using oral tubes. Because of the time required to produce a facial impression with alginate, ie, 5 minutes or even more, the occurrence of movement artifacts is inherent the system.

Digital detection systems which work with laser light or structured white light reduce these movement artifacts by requiring short-measuring times, usually between 1 and 5 seconds.<sup>3,17</sup> State-of-the-art procedures using holography-assisted data acquisition are characterized by ultrashort scan times, in the order of nanoseconds.<sup>18</sup> Such contact-free systems for data acquisition can be used for

recording data even from small children and uncooperative patients.<sup>18</sup> The disadvantages of such high-tech procedures include high equipment purchase costs and the fact that the experimental outlay usually requires the efforts of a specialized team.<sup>18</sup>

In contrast, facial impressioning with alginate offers a low-cost, readily applicable procedure for 3-D facial mapping. Unlike 3-D scanners, extensive overlaying and assembly of facial areas,<sup>17</sup> known as matching, are not required. The resulting facial plaster cast is easily transported and stored. For this reason, facial impressions are used in all fields of medicine, such as in the production of facial epitheses<sup>6</sup> and in radiation protection.<sup>9</sup> In epithetics in particular, the plaster cast must be able to duplicate the 3-D surface of the face as precisely as possible to guarantee optimal fitting of the epithesis. For this reason, a variety of very different modeling techniques have been developed to keep impression errors to a minimum. Apart from impression with alginate,<sup>6</sup> another proven technique is hydrocolloid impression.<sup>8</sup> A further increase in impression and process quality has been achieved using novel computer aided design-computer aided manufacturing (CAD-CAM) procedures<sup>19,20</sup> based on contact-free scanner systems.

## CONCLUSIONS [Return to TOC](#)

- Plaster casts of the facial surface are inadequate for morphometric analyses because the soft facial parts are usually deformed during alginate impression.
- Plaster casts do appear suitable for the 3-D mapping of pathological findings in the face, as in cleft lip and palate patients.
- Additional procedural modifications are necessary to allow the rapid and low-cost procedure of facial impressioning to be used also for 3-D soft tissue analysis in orthodontics.
- A reasonable improvement may arise by impressioning the individual while upright (and not prone) using a stable but nevertheless light, plastic-reinforced alginate bowl to minimize gravity-dependent deformations of the soft facial tissues.

## REFERENCES [Return to TOC](#)

1. Arnett GW, McLaughlin RP. *Facial and Dental Planning for Orthodontists and Oral Surgeons*. Edinburgh, UK: Mosby; 2004:1–12.
2. Schwarz AM. *Lehrgang der Gebissregelung*. Wien, Innsbruck, Austria: Urban und Schwarzenberg 1961;1:121–123.
3. Schwenzer K, Holberg C, Willer J, Mast G, Ehrenfeld M. 3D-Erfassung der Gesichtsoberfläche durch Topometrie unter der Verwendung von projizierten Weißlichtstreifen. *Mund Kiefer GesichtsChir*. 1998; 2:130–134.
4. Ayoub A, Garrahy A, Hood C, White J, Bock M, Siebert JP, Spencer R, Ray A. Validation of a vision-based, three-dimensional facial imaging system. *Cleft Palate Craniofac J*. 2003; 40:523–529.
5. Rommerdale EH. Maxillofacial technology. 1. Introduction to facial impressions. *Trends Tech Contemp Dent Lab*. 1990; 7:436–39.
6. Coleman AJ, Schweiger JW, Urquiola J, Tompkins KA. A two-stage impression technique for custom facial prostheses. *J Prosthet Dent*. 1995; 73:4370–372. [[PubMed Citation](#)]
7. Saunders TR, Hansen NA. Synthetic casting tape as a facial impression tray material. *J Prosthet Dent*. 1995; 74:2169–170. [[PubMed Citation](#)]
8. Lemon JC, Okay DJ, Powers JM, Martin JW, Chambers MS. Facial moulage: the effect of a retarder on compressive strength and working and setting times of irreversible hydrocolloid impression material. *J Prosthet Dent*. 2003; 90:3276–281. [[PubMed Citation](#)]
9. Canup D, Ekstrand KE. A method for the construction of x-ray shielding masks. *Radiol Technol*. 1982; 53:5435–437. [[PubMed Citation](#)]
10. Houston WJ. The analysis of errors in orthodontic measurements. *Am J Orthod*. 1983; 83:382–390. [[PubMed Citation](#)]
11. Farkas LG. *Anthropometry of Head and Face in Medicine*. New York, NY: Elsevier; 1981:1–22.
12. Kawai T, Natsume N, Shibata H, Yamamoto T. Three-dimensional analysis of facial morphology using moiré stripes. Part I: method. *Int J Oral Maxillofac Surg*. 1990; 19:356–358. [[PubMed Citation](#)]
13. Kawai T, Natsume N, Shibata H, Yamamoto T. Three dimensional analysis of facial morphology using moiré stripes. Part II: analysis of normal adults. *Oral Maxillofac Surg*. 1990; 19:359–362.

14. Rasse M, Forkert G, Waldhäusl P. Stereophotogrammetry of facial soft tissue. *Int J Oral Maxillofac Surg.* 1991; 20:163–166. [[PubMed Citation](#)]
15. Ferrario V, Sforza C, Schmitz J, Miani A, Serrao G. A three-dimensional computerized mesh diagram analysis and its application in soft tissue facial morphometry. *Am J Orthod Dentofacial Orthop.* 1998; 114:404–413. [[PubMed Citation](#)]
16. Xia J, Wang D, Samman N, Yeung R, Tideman H. Computer-assisted three-dimensional surgical planning and simulation: 3-D color facial model generation. *Int J Oral Maxillofac Surg.* 2000; 29:2–10. [[PubMed Citation](#)]
17. Holberg C. *Erfassung von Gesichtsoberflächen durch ein lichtcodiertes Triangulationsverfahren* [master's thesis]. Tübingen, Germany: University of Tübingen; 2002.
18. Bongartz J, Giel D, Frey S, Thelen A, Hering P. Hochauflösende dreidimensionale Gesichtsprüfung mit kurzgepulster Holographie. In: Buzug TM, ed. *Physikalische Methoden der Laser- und Medizintechnik*. Düsseldorf, Germany: VDI; 2003:51–56.
19. Chen LH, Tsutsumi S, Iizuka T. A CAD/CAM technique for fabricating facial prostheses: a preliminary report. *Int J Prosthodont.* 1997; 10:5467–472. [[PubMed Citation](#)]
20. Runte C, Dirksen D, Delere H, Thomas C, Runte B, Meyer U, von Bally G, Bollmann F. Optical data acquisition for computer-assisted design of facial prostheses. *Int J Prosthodont.* 2002; 15:2129–132. [[PubMed Citation](#)]

---

**TABLES** [Return to TOC](#)

**TABLE 1.** Definition of the Measuring Points and Their Abbreviations

Soft Tissue Point	Abbreviation	Definition
Forehead	Fo	Between the hairline and the glabella
Glabella	Gl	The most anterior positioned point of the forehead
Soft nasion	N	Point with the smallest radius at the forehead–nasal base transition
Nose tip	Nt	The most anterior point of the nose
Subnasal point	Sn	Point with the least radius at the nose bottom–upper lip transition
Buccal (left)	Bl	Central point of the left cheek
Buccal (right)	Br	Central point of the right cheek
Upper lip	Ls	The most anterior point of the upper lip
Lower lip	Li	The most anterior point of the lower lip
Soft pogonion	Pg	The most anterior point of the soft chin profile
Soft menton	Me	The most caudal point of the soft chin profile

**TABLE 2.** Deviation (in mm) of the Facial Casts at the Measuring Points (n = 15)

Proband No.	Fo	Gl	N	Nt	Sn	Bl	Br	Ls	Li	Pg	Me
1	3.6	4.6	4.9	5.9	5.4	1.9	3.4	5.6	4.5	4.0	6.0
2	1.0	0.0	0.3	4.5	4.4	2.3	2.1	4.2	4.3	5.7	5.0
3	0.7	0.2	0.3	0.4	1.4	3.3	1.8	5.5	9.8	9.8	6.0
4	0.5	0.6	0.3	1.4	0.9	0.8	1.1	1.9	1.8	2.1	2.8
5	0.9	2.1	2.7	4.2	1.1	1.7	2.4	1.1	1.6	3.1	2.9
6	0.0	1.0	1.1	2.4	1.6	1.3	2.1	1.6	0.2	0.4	1.1
7	0.6	0.5	0.0	4.6	3.9	2.2	1.4	4.5	4.2	9.5	9.8
8	1.2	1.4	1.4	5.2	4.8	2.0	3.8	2.8	3.7	3.5	3.4
9	0.6	0.8	2.1	3.2	2.0	1.4	5.2	2.5	2.1	5.8	3.0
10	1.6	1.4	2.1	0.5	1.6	0.6	1.7	2.5	4.5	2.6	2.0
11	1.2	0.1	3.4	6.8	2.7	2.1	2.8	2.0	1.1	0.9	2.4
12	1.1	0.0	0.4	3.0	0.5	1.4	1.0	2.0	0.4	0.9	2.0
13	1.1	0.5	0.5	2.3	1.4	2.5	2.4	3.4	1.4	0.9	2.0
14	0.0	0.2	1.5	2.0	1.6	1.2	0.8	1.6	0.6	1.2	1.0
15	0.4	0.8	0.4	1.2	1.4	1.8	1.7	2.2	1.4	2.9	1.9
Mean	1.0	1.0	1.4	3.2	2.3	1.8	2.3	2.9	2.8	3.6	3.4
SD	0.9	1.2	1.4	2.0	1.6	0.7	1.2	1.4	2.5	3.0	2.4

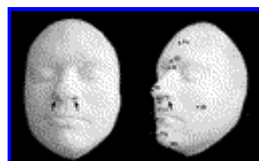
**TABLE 3.** Main Direction of Facial Casts Deviation at the Measuring Points (n = 15)

Direction	Fo	Gl	N	Nt	Sn	Bl	Br	Ls	Li	Pg	Me
Forwards	0	1	0	0	1	1	3	2	0	1	0
Backwards	8	6	2	3	8	3	2	6	8	8	0
Above	0	0	1	3	2	2	1	3	5	4	13
Below	1	2	9	7	4	0	2	4	2	2	2
Inwards	0	0	0	0	0	9	7	0	0	0	0
Outwards	0	0	0	0	0	0	0	0	0	0	0
None	6	6	3	2	0	0	0	0	0	0	0
Total	15	15	15	15	15	15	15	15	15	15	15

**TABLE 4.** Differences Between Nasal and Oral Respiration (in mm)

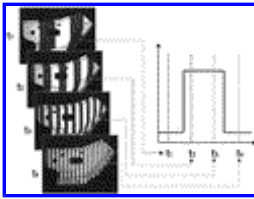
Soft Tissue Point	Abbreviation	Nasal Respiration (n = 12)	Oral Respiration (n = 3)	Total
Forehead	Fo	1.1	0.6	1.0
Glabella	Gl	1.1	0.5	1.0
Nasion	N	1.6	0.8	1.4
Nose tip	Nt	3.3	2.7	3.2
Subnasal point	Sn	2.3	2.4	2.3
Buccal (left)	Bl	1.6	2.3	1.8
Buccal (right)	Br	2.1	2.1	2.3
Upper lip	Ls	2.6	4.2	2.9
Lower lip	Li	2.1	5.4	2.8
Pogonion	Pg	2.4	8.4	3.6
Menton	Me	2.7	6.3	3.4

**FIGURES** [Return to TOC](#)



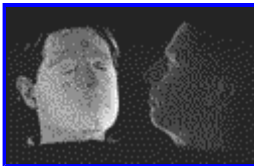
Click on thumbnail for full-sized image.

**FIGURE 1.** Facial plaster cast of a proband. The arrows show the opening for nasal respiration. The measuring points for evaluating the accuracy of the facial casts are shown in the right figure



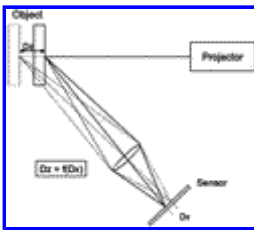
[Click on thumbnail for full-sized image.](#)

**FIGURE 2.** Optimization of coordinate measurement by a space-time coding of individual surface points using phase shifting



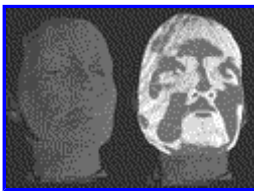
[Click on thumbnail for full-sized image.](#)

**FIGURE 3.** Color-coded point cloud representing the distribution pattern of brightness during three-dimensional (3-D) data acquisition by the 3-D scanner



[Click on thumbnail for full-sized image.](#)

**FIGURE 4.** Principle of optical triangulation. The z-coordinate represents a function of route x at the sensor



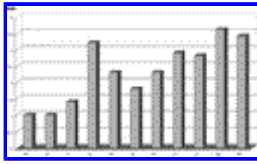
[Click on thumbnail for full-sized image.](#)

**FIGURE 5.** Facial point cloud of a proband (left) matched with the point cloud of his facial plaster cast (right)



[Click on thumbnail for full-sized image.](#)

**FIGURE 6.** Cross sections through the matched point clouds from Figure 5 in a medial (left) and an axial plane (right). One line represents the real face, and the other line represents the facial cast of the proband



Click on thumbnail for full-sized image.

**FIGURE 7.** Mean deviation (n = 15) of the plaster casts at the facial measuring points

<sup>a</sup>Resident, Department of Orthodontics, University of Munich, Munich, Bavaria, Germany

<sup>b</sup>Assistant Professor, Department of Maxillofacial Surgery, University of Basel, Basel, Switzerland

<sup>c</sup>Resident, Department of Orthodontics, University of Munich, Munich, Bavaria, Germany

<sup>d</sup>Department Head, Department of Orthodontics, University of Munich, Munich, Bavaria, Germany

Corresponding author: Dr. Christof Holberg, Department of Orthodontics, University of Munich, Goethestrasse 70, Munich, Bavaria 80336, Germany (E-mail: [christof.holberg@med.uni-muenchen.de](mailto:christof.holberg@med.uni-muenchen.de))